Available online at www.sciencedirect.com
SCIENCE DIRECT
Thin Solid Films 493 (2005) 319 – 324
thin solid films
www.elsevier.com/locate/tsf

Light-intensity dependence of the steady-state photoconductivity used to estimate the density of states in the gap of intrinsic semiconductors

J.A. Schmidt [a,b,*], C. Longeaud [c], J.P. Kleider [c]

[a] INTEC (UNL-CONICET), Güemes 3450, 3000 Santa Fe, Argentina
[b] FIQ (UNL), Santiago del Estero 2829, 3000 Santa Fe, Argentina
[c] Laboratoire de Génie Electrique de Paris, (UMR 8507 CNRS) Ecole Supérieure dElectricité, Université Paris VI et XI, Plateau de Moulon, 91192 Gif-sur-Y vette CEDEX, France

Received 1 February 2005; received in revised form 31 May 2005; accepted 7 August 2005
Available online 26 September 2005

Abstract

We present a method to obtain the density of states of photoconductive semiconductors based on the light-intensity dependence of the steady-state photoconductivity. A simple expression—relating the density of states at the electron quasi-Fermi level to measurable quantities—is deduced by performing suitable approximations from the analytical solution of the generalized equations that describe the photoconductivity of semiconductors. The validity of the approximations and the applicability of the final expression are verified from numerical simulations of the process. The usefulness of the method is demonstrated by performing measurements on a standard hydrogenated amorphous silicon sample.

PACS: 72.20.Jv; 72.40.+w; 72.80.Ng
Keywords: Semiconductors; Photoconductivity; Density of states; Electrical properties and measurements

1. Introduction

The steady-state photoconductivity is one of the most widely studied properties of semiconductors. Light absorption increases the concentration of free carriers, whose lifetime is ultimately limited by recombination. Except for pure single crystalline semiconductors, a considerable density of localized states within the forbidden gap is known to exist. These defect states are usually the most efficient recombination centers which determine the transport properties and the photoconductivity. Therefore, many papers in the literature concern the photoconductivity and its dependence upon light flux or generation rate, with the aim to derive defect parameters of the material. For different semiconductor materials, like CdS, Sb_2S_3 or hydrogenated amorphous silicon (a-Si:H), a power-law dependence of the photoconductivity σ_{ph} on the light flux Φ has been observed: $\sigma_{ph} \propto \Phi^{\gamma}$. Several models have been proposed to explain this odd behavior of the photoconductivity, and to try to correlate the γ exponent to some part of the density of states (DOS) of the material. Rose [1] was the first to show that in an exponentially varying DOS, the exponent would be given by $\gamma = T_C/(T+T_C)$, where T is the temperature and T_C is the characteristic temperature that describes the exponentially decreasing conduction band tail. Following the work of Rose, many authors investigated the γ exponent in a-Si:H and commented on the link with the DOS [2–7]. While some authors suggested the possibility to estimate the DOS as a function of energy directly from photoconductivity measurements [4], other authors concluded that the γ coefficient is more sensitive to the total number of defects rather than to their distribution [7], thus throwing doubt on the possibility to develop a DOS spectroscopy from the dependence of the γ coefficient.

In this work we show that a DOS spectroscopy is indeed possible by using the dependence of the γ coefficient upon the temperature and the light flux, and we illustrate this concept on the basis of both numerical calculations and experimental results.

* Corresponding author. INTEC (UNL-CONICET), Güemes 3450, 3000 Santa Fe, Argentina.
E-mail address: jschmidt@intec.unl.edu.ar (J.A. Schmidt).

0040-6090/$ - see front matter © 2005 Elsevier B.V. All rights reserved.
doi:10.1016/j.tsf.2005.08.060

2. Theoretical background

We will consider an arbitrary distribution of defect states throughout the gap of the semiconductor, characterized by the DOS function $N(E)$. When the solid is uniformly illuminated with photons of energy larger than the band gap, a constant generation rate per unit volume G of electron-hole pairs will result. Simmons and Taylor [8] have described the non-equilibrium steady-state statistics for such an arbitrary distribution of gap states. In the steady-state, the optical generation rate is balanced by recombination, according to the following rate equations:

$$\frac{\mathrm{d}n}{\mathrm{d}t} = 0 = G - \int_{E_V}^{E_C} c_n n[1-f(E)]N(E)\mathrm{d}E + \int_{E_V}^{E_C} e_n(E)f(E)N(E)\mathrm{d}E - \beta np, \quad (1)$$

$$\frac{\mathrm{d}p}{\mathrm{d}t} = 0 = G - \int_{E_V}^{E_C} c_p f(E)N(E)\mathrm{d}E + \int_{E_V}^{E_C} e_p(E)[1-f(E)]N(E)\mathrm{d}E - \beta np, \quad (2)$$

where n and p are the concentrations of electrons and holes in extended states, c_n and c_p are the capture coefficients, $e_n(E)$ and $e_p(E)$ are the emission coefficients for electrons and holes, respectively, t is the time, E_V is the energy at the top of the valence band, E_C is the energy at the bottom of the conduction band, $f(E)$ is the occupation function, and the term βnp is the rate of bimolecular recombination, which we will assume in the following to be much lower than the rate of recombination through localized states. As remarked in Ref. [8], if all the states belong to a single species of traps, so that the ratio c_n/c_p is energy-independent, a single occupation function describes the occupancy of all the traps,

$$f(E) = \frac{c_n n + e_p(E)}{c_n n + c_p p + e_n(E) + e_p(E)}. \quad (3)$$

Replacing Eq. (3) into Eq. (2) we get $G = \int_{E_V}^{E_C}\left[\frac{c_n n c_p p - e_n(E)e_p(E)}{c_n n + c_p p + e_n(E) + e_p(E)}\right]N(E)\mathrm{d}E$, which can be approximated to give [9]

$$G = \int_{E_{tp}}^{E_{tn}}\left[\frac{c_n n c_p p}{c_n n + c_p p}\right]N(E)\mathrm{d}E, \quad (4)$$

where E_{tn} and E_{tp} are the quasi-Fermi levels for trapped electrons and holes, respectively.

On the other hand, the condition of charge conservation between dark equilibrium and steady-state under illumination gives the following condition

$$n_0 - p_0 + \int_{E_V}^{E_C} f_0(E)N(E)\mathrm{d}E = n - p + \int_{E_V}^{E_C} f(E)N(E)\mathrm{d}E, \quad (5)$$

where the subscript "zero" stands for dark equilibrium values. In defective semiconductors, where the concentration of excess free carriers is negligible compared to the concentration of trapped carriers, the terms $(n_0 - p_0)$ and $(n-p)$ can be neglected compared to the integrals in Eq. (5). This is true even for device-quality a-Si:H [5]. Moreover, in a low-temperature approximation we have that $f(E) \approx 0$ for $E > E_{tn}$; $f(E) \approx c_n n/(c_n n + c_p p)$ for $E_{tp} < E < E_{tn}$; and $f(E) \approx 1$ for $E > E_{tp}$. Following the work of Taylor and Simmons [9] and combining Eqs. (4) and (5) with the preceding approximate expressions for $f(E)$, after some easy calculations we can write

$$G = \frac{n}{\tau_n} \approx c_n n \int_{E_{F0}}^{E_{tn}} N(E)\mathrm{d}E, \quad (6)$$

and, as well, $G = \frac{p}{\tau_p} \approx c_p p \int_{E_{tp}}^{E_{F0}} N(E)\mathrm{d}E$, where $\tau_n(\tau_p)$ is the free electron (hole) lifetime and E_{F0} is the dark equilibrium Fermi level. Without lost of generality we will consider in the following a semiconductor where electrons are the majority carriers, so that $n \gg p$ and $c_n n \gg c_p p$, and we will derive a simple expression relating the DOS at E_{tn} to measurable quantities. If holes were the dominant type of carriers, a similar relation could be derived for the DOS at E_{tp}. Under this assumption of n-type character, the photoconductivity can be approximated by $\sigma_{ph} \cong q\mu_n(n - n_0)$, where μ_n is the mobility of the electrons in the extended states. Also, the quasi-Fermi level for trapped electrons is almost equal to that for free electrons, E_{Fn},

$$E_{tn} \approx E_{Fn} = E_{F0} + k_B T \ln\left(\frac{n}{n_0}\right), \quad (7)$$

where k_B is the Boltzmann's constant and T is the absolute temperature.

Thus, Eq. (6) expresses the generation rate as a function of n. By taking the logarithmic derivative, we get

$$\frac{\mathrm{d}(\ln G)}{\mathrm{d}(\ln n)} = 1 + \frac{c_n n}{G}\frac{\mathrm{d}}{\mathrm{d}E_{Fn}}\left[\int_{E_{F0}}^{E_{Fn}} N(E)\mathrm{d}E\right]\frac{\mathrm{d}E_{Fn}}{\mathrm{d}(\ln n)} = 1 + \frac{c_n n}{G}N(E_{Fn})k_B T. \quad (8)$$

Defining the parameter γ_n as

$$\gamma_n^{-1} = \frac{\mathrm{d}(\ln G)}{\mathrm{d}(\ln n)}, \quad (9)$$

from the combination of Eqs. (8) and (9) we obtain the very simple expression $N(E_{Fn}) = \frac{G}{k_B T c_n n}\left[\frac{1}{\gamma_n} - 1\right]$. Since under the usual illumination conditions $n \gg n_0$, we have $\sigma_{ph} \cong q\mu_n n$, and hence

$$N(E_{Fn}) = \frac{q\mu_n G}{k_B T c_n \sigma_{ph}}\left[\frac{1}{\gamma_n} - 1\right]. \quad (10)$$

Eq. (10) expresses the DOS at the quasi-Fermi energy as a function of material parameters (c_n and μ_n) and experimental magnitudes that can be easily measured (temper-

ature, generation rate, photoconductivity, and γ_n). The quasi-Fermi energy E_{Fn} can be evaluated from σ_{ph} as $E_{Fn}=E_c-k_BT\ln\left[\frac{q\mu_n k_B T N(E_c)}{\sigma_{ph}}\right]$, and it can be varied either from a temperature scan or a generation rate scan. That gives the basis for a DOS spectroscopy in the upper half of the band gap. Note that Eq. (9) defines the γ_n coefficient locally around the G value that determines the photoconductivity. For an exponentially varying DOS, the γ_n coefficient is constant over decades of the generation rate [1], while for other DOS distributions it may depend on G. However, our analysis is independent of a peculiar DOS shape and valid regardless of the constancy of γ_n.

3. Results and discussion

To test the applicability of our method we have performed a numerical simulation of the experiment, starting from a typical DOS for hydrogenated amorphous silicon (Fig. 1, lines). We have assumed equal values for the DOS at the band edges, $N(E_C)=N(E_V)=10^{21}$ cm^{-3} eV^{-1}, band tails of characteristic temperatures $T_C=250$ K and $T_V=600$ K, and Gaussian defect distributions with a standard deviation of $\sigma=150$ meV. We have taken standard values for the material parameters, like the extended-states mobilities $\mu_n=10$ cm^2 V^{-1} s^{-1} and $\mu_p=1$ cm^2 V^{-1} s^{-1} obtained from time-of-flight experiments [10], and the capture coefficients $c_n=2\times10^{-8}$ cm^3 s^{-1} and $c_p=1\times10^{-8}$ cm^3 s^{-1} also deduced from time-of-flight measurements [11]. We have solved numerically the continuity and charge neutrality equations [Eqs. (1), (2) and (5)] to obtain the steady-state densities of free electrons and holes at each temperature and generation rate, computing then the photoconductivity as $\sigma_{ph}(T,G)=q\mu_n[n(T,G)-n_0(T)]+q\mu_p[p(T,G)-p_0(T)]$.

First of all, we would like to show that the model calculations that we are using reproduce the experimentally

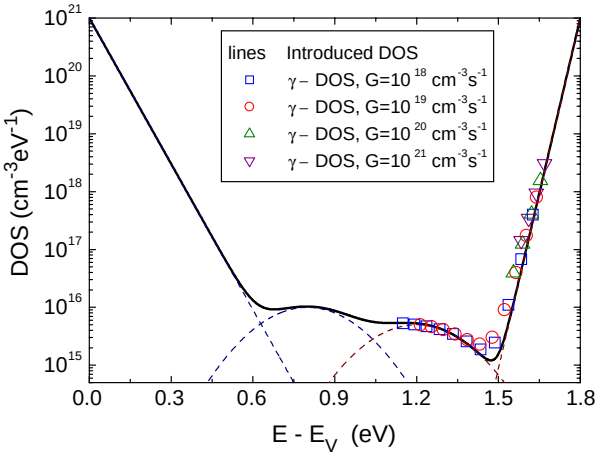

Fig. 1. Comparison between the introduced DOS (lines) and the DOS calculated from Eq. (10) for different temperatures and generation rates (symbols).

measured behavior of the photoconductivity. A very stringent requirement for a model that attempts to describe the photoconductivity behavior has been proposed by I. Balberg [3]. The requirement is based on the analysis of four phototransport properties as a function of temperature, namely the two carriers mobility-lifetime products $\mu_n\tau_n$ and $\mu_p\tau_p$, and their light intensity exponents γ_n and γ_p, where the first coefficient is the same that we have already defined in Eq. (9), or equivalently as $\mu_n\tau_n \propto G^{(\gamma_n-1)}$, and the second coefficient is defined from $\mu_p\tau_p \propto G^{(\gamma_p-1)}$. The solution of the steady-state continuity and charge neutrality equations, which provides the electrons and holes densities at each temperature and generation rate, allows us to obtain the model-computed temperature dependencies of $\mu_n\tau_n$, $\mu_p\tau_p$, γ_n and γ_p. These values are calculated as $\tau_n=\frac{(n-n_0)}{G}$, $\tau_p=\frac{(p-p_0)}{G}$, $\gamma_n=1+\frac{G}{\mu_n\tau_n}\frac{\delta(\mu_n\tau_n)}{\delta G}$, $\gamma_p=1+\frac{G}{\mu_p\tau_p}\frac{\delta(\mu_p\tau_p)}{\delta G}$ where $\delta(\mu_n\tau_n)$ and $\delta(\mu_p\tau_p)$ are the (small) variations of the mobility-lifetime products for electrons and holes caused by a very small change δG of the generation rate. These four computed phototransport properties can be compared to the experimental results obtained by us and by other authors [3,5,12,13]. The computed dependence is shown in Fig. 2(a)–(d) as circles. In Fig. 2(a) and (b) we also present our own experimental results for $\mu_n\tau_n$ and γ_n as triangles (the experimental conditions will be described below). Although a disagreement between our calculations and the experimental results can be appreciated, we would like to clarify that our intention is not to fit our experimental results, but rather to show that the main experimental trends are well reproduced by our simulation. The results of our calculations can also be compared with other typical measurements on a-Si:H samples, like the ones presented in Fig. 1 of Ref. [3]. This comparison shows that once again the main features of the measured behavior are well described. The mobility-lifetime product for electrons $\mu_n\tau_n$ is approximately constant up to $1000/T\sim5$ K^{-1}, then decreasing strongly as the temperature decreases further, just like typically measured values (see also Ref. [5]). The mobility-lifetime product for holes $\mu_p\tau_p$ shows a monotonic decrease as the temperature decreases, tending gradually towards a constant value for low temperatures, also in agreement with typical measurements [12,13]. The calculated γ_n coefficient exhibits a maximum around $1000/T\sim4$ K^{-1} as the measured one. Note that the present values for the parameters introduced in our calculations do not give the supralinear behavior measured in some a-Si:H samples. With other values for the capture coefficients, particularly introducing two species of traps, we have been able to reproduce the larger-than-unity γ_n values.

Concerning the behavior of γ_p, we would like to comment on the experimental procedure used to extract this coefficient. What is measured experimentally [3,12,13] is the light-intensity dependence of the ambipolar diffusion length (L_{amb}) as obtained from steady-state photocarrier grating (SSPG) measurements. The accurate determination of L_{amb} from SSPG data is still a matter of debate, but it

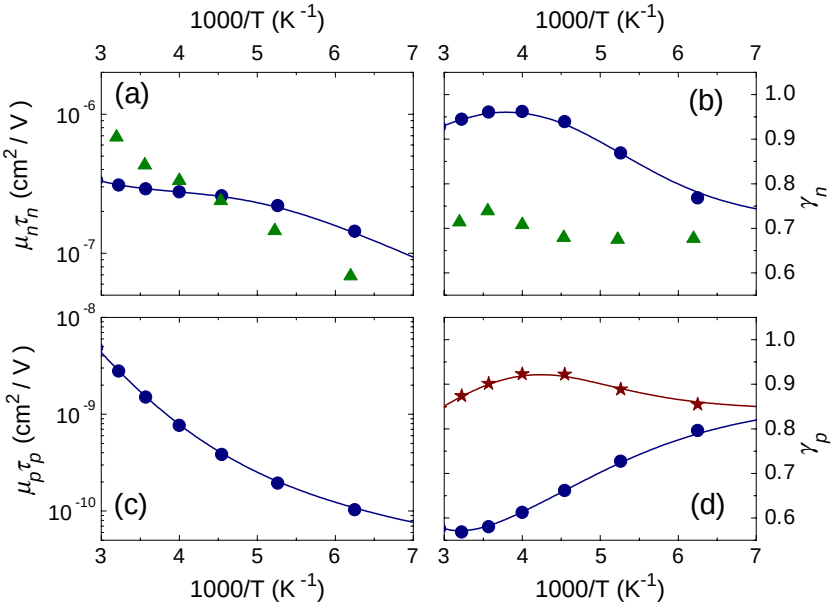

Fig. 2. Model-computed temperature dependence (circles) of the four phototransport properties arising from a "sample" with the DOS shown in Fig. 1. All the values have been calculated for a generation rate around 10^{20} $cm^{-3}s^{-1}$. In (d) we present the γ_p values calculated by using two different procedures (see text for discussion). Lines are guides to the eye. In (a) and (b) we also present for comparison the experimental results obtained in our sample (triangles).

seems to be clear that the formula originally proposed by Ritter, Zeldov and Weiser (RZW) [14,15] is not accurate enough. Hattori et al. [16] have shown that a fit with this formula provides an apparent diffusion length that can even have a light-intensity dependence opposite to the real one. Based on the solution of the complete equations that describe the SSPG phenomenon, we have recently obtained similar results showing that the method cannot be trusted [17]. In Fig. 2(d) we show as stars the γ_p coefficient that would be obtained "experimentally" from the light-intensity dependence $L_{amb} \propto G^{(\gamma_p-1)/2}$ (as done in Ref. [3]), where L_{amb} is in turn obtained by fitting the numerically calculated SSPG curves with the RZW formula. On the other hand, the circles of Fig. 2(d) show the γ_p coefficient that is calculated from $\mu_p\tau_p \propto G^{(\gamma_p-1)}$, where $\mu_p\tau_p$ is obtained as described above from the numerical solution of the steady-state transport equations. As can be seen, the behavior of both curves is quite dissimilar, meaning that trying to extract the DOS from a fit of the $\gamma_p(T)$ curve (obtaining γ_p from a fit of SSPG results with the RZW formula) can lead to completely erroneous results. For that reason, we consider that a better approach to estimate the DOS is to use a formula like Eq. (10), which directly links the DOS to measurable quantities.

Coming back to the procedure that we have used to test our method for DOS evaluation, we have worked on the simulated results as we would have treated the experimental data. We have calculated the γ_n coefficient from the steady-state photoconductivity, changing the generation rate in ±5% relative to each central value. E_{Fn} has been calculated from Eq. (7), where we have approximated the ratio n/n_0 by the ratio between the photoconductivity and the dark conductivity. Then we applied Eq. (10) to reconstruct the DOS, changing E_{Fn} from a variation of T and G. In Fig. 1 the symbols show the reconstruction of the initially introduced DOS. As can be seen, Eq. (10) is able to reconstruct the DOS with excellent accuracy over a wide energy range. Similar results have been obtained from several simulations for different DOSs.

In order to show that the method is not limited to amorphous materials, we performed a simulation starting from a DOS representing a possible distribution for a crystalline material with some defect levels in the gap (Fig. 3, lines). The defect states are represented by Gaussian functions having a width of 50 meV, with capture coefficients $c_n = 2\times10^{-8}$ cm^3 s^{-1} and $c_p = 1\times10^{-8}$ cm^3 s^{-1}. The equilibrium (dark) Fermi level that ensures charge neutrality for this DOS lies at 1 eV. As before, we solved numerically the continuity and charge neutrality equations to obtain the photoconductivity and the γ_n coefficient as a

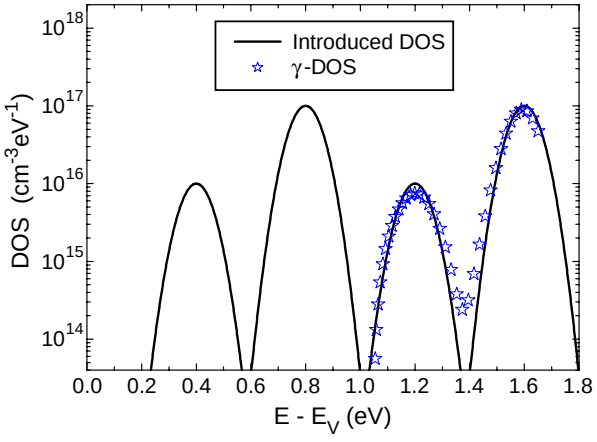

Fig. 3. DOS reconstruction from Eq. (10) for a crystalline-like DOS.

function of temperature, and we applied Eq. (10) to calculate the DOS at the electron quasi-Fermi level. The result is also shown in Fig. 3 (stars), where it can be seen that the γ-DOS follows the introduced DOS with a remarkable accuracy.

4. Experimental details

To prove the experimental usefulness of the technique, preliminary measurements on a hydrogenated amorphous silicon sample have been made. Note that according to Eq. (10) we do not obtain directly the density of states from the experimental data, but rather the quantity $N(E_{\mathrm{tn}}) \times c_n/\mu_n$. This quantity is also obtained from the modulated photocurrent (MPC) technique performed in the high frequency range and from the recently proposed method to extract the DOS from SSPG measurements [17,18]. Thus, the validity of the γ-DOS determination can be confirmed by comparing it to the MPC-DOS and SSPG-DOS obtained on the same a-Si:H sample by using the same standard values for c_n and μ_n.

We applied the new technique to a standard hydrogenated amorphous silicon sample prepared under conditions described elsewhere [19]. The sample has a thickness of 0.65 μm, a room-temperature dark conductivity of $6.5 \times 10^{-8}\ \Omega^{-1}\ \mathrm{cm}^{-1}$ and an activation energy of 0.62 eV. We deposited parallel coplanar aluminum contacts 1 mm apart, and we measured the photoconductivity and the γ_n coefficient as functions of temperature. Measurements were performed under vacuum, with a pressure lower than 10^{-5} Torr. We performed a temperature scan from 100 to 370 K in 30 K steps, at a fixed generation rate $G = 2 \times 10^{21}\ \mathrm{cm}^{-3}\ \mathrm{s}^{-1}$. The behavior of $\mu_n\tau_n$ and γ_n as a function of the inverse temperature has already been presented in Fig. 2 (triangles). The application of Eq. (10) to these data is shown in Fig. 4, where our new technique based on the γ coefficient is compared with the MPC methods, performed on the same sample both in the high frequency (HFMPC) [20] and the low frequency (LFMPC) [21] limits, and with the SSPG-DOS method [17,18]. Note that energies are now referred to the conduction band edge to avoid uncertainties in the value of the mobility gap of the sample. For the HFMPC method, each curve corresponds to a frequency scan performed at a different temperature. As demonstrated in Ref. [20], the actual DOS is reproduced by the upper envelope of all the frequency scans performed at different temperatures. The maxima exhibited by the curves at low temperatures (low energies) are due to a bad signal to noise ratio appearing at high frequencies, i.e., when the DOS is high and the sample response is proportionally low. The departure of the curves from the upper envelope at high temperatures (high energies) results from the influence of the continuous flux used in the method. For a detailed discussion of the HFMPC method, and in particular on the DOS shape determination, the reader is referred to Ref. [20].

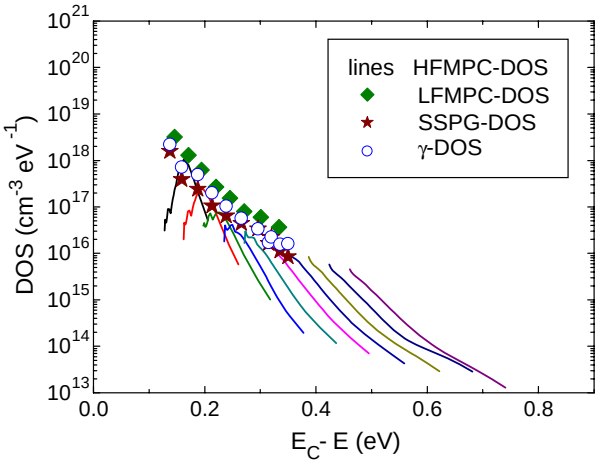

Fig. 4. Comparison between DOS determinations on the same a-Si:H sample from modulated photoconductivity in the high frequency (HFMPC) and low frequency (LFMPC) regimes, from steady-state photocurrent grating (SSPG) measurements, and from γ-coefficient measurements. For HFMPC data, each line corresponds to a frequency scan performed at a different temperature (see text).

To obtain absolute DOS values, an electron mobility $\mu_n = 10\ \mathrm{cm}^2\ \mathrm{V}^{-1}\ \mathrm{s}^{-1}$ and a capture coefficient $c_n = 10^{-8}\ \mathrm{cm}^3\ \mathrm{s}^{-1}$ have been assumed in all the methods. Other values for these parameters would essentially shift the HFMPC-DOS, SSPG-DOS and γ-DOS curves vertically, without significantly changing the shapes and with only a slight change in the energy position (see below). The LFMPC-DOS curve, however, would not be affected, since this method provides directly the DOS distribution [21]. Therefore, the close agreement between the methods shown in Fig. 4 allows us to ensure that the c_n/μ_n ratio is close to 10^{-9}V cm for this sample. To set the energy scale we have used $E_{\mathrm{tn}} \approx E_{\mathrm{Fn}} = E_{\mathrm{c}} - k_{\mathrm{B}}T \ln\left[\frac{q\mu_n k_{\mathrm{B}} T N(E_{\mathrm{c}})}{\sigma_{\mathrm{ph}}}\right]$ for γ-DOS, SSPG-DOS and LFMPC-DOS (see Ref. [21]), and $E_{\omega n} = E_{\mathrm{c}} - k_{\mathrm{B}}T \ln\left[\frac{c_n k_{\mathrm{B}} T N(E_{\mathrm{c}})}{\omega}\right]$ for HFMPC-DOS (see Ref. [20]), where the pulsation of the excitation was varied in the range $10^2\ \mathrm{s}^{-1} \le \omega \le 6 \times 10^5\ \mathrm{s}^{-1}$. The preceding equations show that the energy scale of the HFMPC-DOS is affected by the value of c_n but not by the value of μ_n, while for the other methods the reverse is true, the energy scale is affected by μ_n and not by c_n. Consequently, the very good agreement between the methods shown in Fig. 4 is an indication that the individual values of $c_n = 10^{-8}\ \mathrm{cm}^3\ \mathrm{s}^{-1}$ and $\mu_n = 10\ \mathrm{cm}^2\ \mathrm{V}^{-1}\mathrm{s}^{-1}$ are good estimates for the values of these parameters, and at the same time give us confidence on the new technique. A fit of the band-tail region with an exponential function gives a characteristic energy of 23±2 meV, meaning a characteristic temperature of 270 K, in agreement with previous determinations [22]. The present temperature variation from 100 to 370 K provides a DOS reconstruction over an energy range of ~0.25 eV, which can be further expanded performing experiments as a function of the generation rate (see Fig. 1). We would

like to stress the simplicity of the DOS estimations from measurements of the γ coefficient as a function of temperature, since only steady-state photoconductivity measurements are needed. The experimental technique is really straightforward, and the accuracy of the DOS determination is comparable to the one of the MPC and SSPG techniques.

Our preceding analysis assumes a single species of traps within the gap of the semiconductor. When different species of traps are present, Eq. (10) is no longer valid and it has to be replaced by a more complex expression. Obviously, a supralinear dependence of the photoconductivity on the generation rate ($\gamma > 1$), such as the one observed in some a-Si:H samples at low temperatures, would cause Eq. (10) to give unreasonable negative values. This sensitization effect, however, appears when different species of traps are present, a situation that is not considered in the simple treatment that we present in this paper. The case of different species of traps will be treated in detail elsewhere.

5. Conclusion

In conclusion, we have developed an extremely simple method for DOS determinations in photoconductive semiconductors based on measurements of the light-intensity dependence of the steady-state photoconductivity. The DOS could in principle be evaluated between the dark Fermi level and the conduction band edge, and is obtained in the form of the $c_n N/\mu_n$ product, meaning that to get absolute DOS values it is required to know the values of the capture coefficient and the electron mobility. A good order of magnitude for these parameters can be obtained when using this method in combination with other techniques (like MPC) that also provide DOS estimations over the same energy range. We have performed simulations starting from DOS distributions typical for amorphous and crystalline materials, and we have shown that the method is able to reproduce the introduced DOS. We have presented preliminary measurements on an a-Si:H sample, which demonstrate that the method is applicable, experimentally simple, and capable of providing DOS determinations compatible with the ones obtained from the modulated photoconductivity and steady-state photocarrier grating methods.

Acknowledgements

This work was partly supported by ECOS Sud-SECyT (project A02E01). J.A.S. also acknowledges support from CONICET (PEI N° 6329) and the Alexander von Humboldt Foundation.

References

[1] A. Rose, Concepts in Photoconductivity and Allied Problems, 2nd edition, Robert E. Krieger Publishing CO., Huntington, 1978, p. 41.
[2] J.Z. Liu, S. Wagner, Phys. Rev., B 39 (1989) 11156.
[3] I. Balberg, J. Non-Cryst. Solids 299–302 (2002) 531.
[4] D. Mendoza, W. Pickin, Phys. Rev., B 40 (1989) 3914.
[5] M.Q. Tran, Philos. Mag., B 72 (1995) 35.
[6] Y. Almeriouh, J. Bullot, P. Cordier, M. Gauthier, G. Mawawa, Philos. Mag., B 63 (1991) 1015.
[7] D.S. Shen, S. Wagner, J. Appl. Phys. 78 (1995) 278.
[8] J.G. Simmons, G.W. Taylor, Phys. Rev., B 4 (1971) 502.
[9] G.W. Taylor, J.G. Simmons, J. Non-Cryst. Solids 8–10 (1972) 940.
[10] T. Tiedje, in: J. Pankove (Ed.), Semiconductors and Semimetals, 21C, Academic Press, New York, 1984, p. 207.
[11] R. Vanderhaghen, Phys. Rev., B 38 (1988) 10755.
[12] Y. Lubianiker, I. Balberg, L.F. Fonseca, Phys. Rev., B 55 (1997) R15997.
[13] R. Rapaport, Y. Lubianiker, I. Balberg, L. Fonseca, Appl. Phys. Lett. 72 (1998) 103.
[14] D. Ritter, E. Zeldov, K. Weiser, Appl. Phys. Lett. 49 (1986) 791.
[15] D. Ritter, K. Weiser, E. Zeldov, J. Appl. Phys. 62 (1987) 4563.
[16] K. Hattori, H. Okamoto, Y. Hamakawa, Phys. Rev., B 45 (1992) 1126.
[17] J.A. Schmidt, C. Longeaud, Phys. Rev., B 71 (2005) 125208.
[18] J.A. Schmidt, C. Longeaud, Appl. Phys. Lett. 85 (2004) 4412.
[19] R.H. Buitrago, R. Arce, R.R. Koropecki, J. Non-Cryst. Solids 164–166 (1993) 259.
[20] C. Longeaud, J.P. Kleider, Phys. Rev., B 45 (1992) 11672.
[21] R.R. Koropecki, J.A. Schmidt, R. Arce, J. Appl. Phys. 91 (2002) 9865.
[22] R.A. Street, Hydrogenated Amorphous Silicon, Cambridge University Press, Cambridge, 1991, p. 81, see for example.